Photoactivation of the Photosynthetic Reaction Center of *Blastochloris viridis* in the Crystalline State

Richard H. G. Baxter,*,† Elmars Krausz,‡ and James R. Norris†

Department of Chemistry, University of Chicago, 5735 South Ellis Avenue, Chicago, Illinois 60637, and Research School of Chemistry, Australian National University, Canberra ACT 0200, Australia

Received: July 6, 2005; In Final Form: October 28, 2005

Photoactivation in crystals of the bacterial reaction center of *Blastochloris viridis* was investigated by near-infrared spectroscopy. The bleaching of the special pair absorption at 970 nm and the simultaneous rise of the special pair cation absorption at 1300 nm were measured in response to transient irradiation by a HeNe laser over 5 orders of magnitude in laser power. The resulting power-saturation curve can be used to estimate the true extent of photoactivation achieved in a prior time-resolved crystallographic experiment (Baxter et al. *Proc. Natl. Acad. Sci. U.S.A.* **2004**, *101*, 5982−5987). The overall extent of photoactivation was 50%, which demonstrates that the time-resolved crystallographic method can be applied to the optically dense reaction center crystals. Measurement of the charge-recombination rate, however, suggests the presence of a long-lived P^+ state within the crystal.

Introduction

The photosynthetic reaction center is an integral membrane protein that is responsible for the primary act of photosynthesis: the conversion of light energy into chemical energy.[1] This is achieved by a series of optimized electron-transfer reactions between chromophores bound to the protein,[2] resulting in the separation of charge across a biological membrane. The primary donor (P) in the reaction center (RC) is a special pair of bacteriochlorophyll molecules bound by the protein to form an electronically coupled dimer near the periplasmic side of the membrane. Upon excitation by light, the special pair donates an electron to a nearby bacteriopheophytin (BPh_A) with a time constant of ∼3 ps at room temperature[3] and becomes a cation (P^+). Further electron transfer occurs from BPh_A to a primary quinone acceptor (Q_A) with a time constant of ∼200 ps at room temperature[3] and then to a secondary quinone acceptor (Q_B). Q_B is a ubiquinone that binds to an active site near the cytoplasmic side of the membrane. While in its active site, Q_B accepts two electrons and two cytoplasmic protons, becoming reduced to dihydroquinol, then leaves the active site to a membrane-soluble quinone pool.

The RC of the purple non-sulfur bacterium *Blastochloris* (formerly *Rhodopseudomonas*) *viridis* was the first integral membrane whose structure was determined by X-ray crystallography.[4] In the original model of the *B. viridis* RC, Q_B was positioned relatively deep within its binding pocket, within hydrogen-bonding distance of the residue His L190. A second position for the quinone was observed in trigonal crystals of the RC from *Rhodobacter sphaeroides* that was displaced 5 Å toward the solvent and rotated 180° with respect to its isoprenoid tail.[5] These two positions have been labeled the "proximal" and the "distal" sites, respectively.[6] Recent structures of the RC from both *B. viridis* and *R. sphaeroide*s have observed the quinone to occupy either or both of these positions,[6−16] and the site preference of Q_B has been variously attributed to the presence of quinol in place of quinone,[5] differing isoprenyl chain length,[6] electronic state (Q_B vs Q_B^-),[7] protonation of ionizable residues within the Q_B pocket,[17] and the temperature and/or influence of cryoprotectants used during data collection.[14]

The first electron transfer from Q_A to Q_B is believed to involve a "conformational gate".[18] Electron transfer from Q_A to Q_B does not proceed in RCs of *R. sphaeroides* frozen in darkness but does in RCs frozen under illumination,[19] and the rate of electron transfer is independent of the free energy of the reaction.[20] On the basis of a crystallographic freeze-trapping study in *R. sphaeroides*, a hypothesis has been presented in which the movement of Q_B from the distal to the proximal position was the rate-limiting step for secondary electron transfer.[7] To test this hypothesis in *B. viridis*, a time-resolved crystallographic experiment was conducted in which the structure of the reaction center was determined with a time resolution of several milliseconds before and after illumination of the crystal with a pulsed laser.[21] No significant difference was observed between the light and the dark states, in agreement with the results of Fourier transform infrared (FTIR) difference spectroscopy in *R. sphaeroides* reaction centers.[22−24] This experiment implied that the movement of Q_B from the distal to the proximal position was not reversible on the time scale of the experiment, i.e., the dark period of ∼6 s.[21]

Besides addressing the hypothesis of conformational gating, the time-resolved crystallographic experiment represented a significant extension of the technique of time-resolved crystallography to a large, integral membrane protein, and a crystal of significantly greater optical density in comparison to previously studied crystals of myoglobin[25,26] or photoactive yellow protein (PYP).[27−29] Two important assumptions underpin the result of this experiment: first, that the laser illumination system was sufficient to generate significant photoactivation within the crystal, and second, that the photoactivated centers relaxed to

* Author to whom correspondence should be addressed. Present address: Howard Hughes Medical Institute Research Laboratories, University of Texas Southwestern Medical Center, 6001 Forest Park Road, Dallas, TX 75390-9050, Phone: (214) 645-5943. Fax: (214) 645-5945. E-mail: rbaxter@alumni.uchicago.edu.

† University of Chicago.

‡ Australian National University.

10.1021/jp053697p CCC: $33.50
Published on Web 12/18/2005

the ground state in the time between laser pulses. Although estimates of the extent of photoactivation and the rate of charge recombination are possible based on results from studies of reaction centers in solution, it is preferable to verify these estimates in the crystalline state and under conditions as close as possible to the actual crystallographic experiment. Here, we test the assumptions regarding photoactivation of reaction center crystals using optical spectroscopy.

Ideally, one would monitor the extent of photoactivation simultaneously with the X-ray exposure during the time-resolved experiment. The multiple demands for space around the crystal during X-ray data collection, however, make this a considerable technical challenge. A number of microcrystal spectrophotometers have been reported,[30] including those designed to operate in situ.[31−33] In the case of reaction center crystals, however, there is a fundamental incompatibility in the sample size for crystallographic data collection, for which the X-ray scattering power is proportional to volume, and the sample size appropriate for accurate microspectrophotometry, which becomes problematic for optical densities greater than 2.[34] Hence, we selected small crystals for off-line spectroscopic study, including measurement of the P^+ absorption band in the near-infrared. Estimations of photoactivation within *R. sphaeroides* crystals[7] and the kinetics of electron transfer between Q_A and Q_B[10] have been made previously. The optical spectra of *B. viridis* crystals have been previously reported,[35,36] but not their spectra in the near-infrared or the measurement of kinetics within the crystal.

Materials and Methods

RCs were purified from *B. viridis* cells (ATCC 19567) in a rich medium originally devised for cultures of *R. capsulatus*.[37] Approximately 16 L of culture was grown in 4 × 4 L stirred flasks on a purpose-built shelf under semi-anaerobic conditions. Illumination was provided by a set of tungsten bulbs, which also produced an ambient temperature of 28−32 °C. Reaction centers were isolated, purified, and crystallized as previously described.[6,38,39] Final purity was judged by $A_{280}/A_{830} < 2.1$. Crystals grew in 1−3 weeks in 1.8−2.1 M ammonium sulfate (ACS grade, Aldrich, Milwaukee, WI), 0.1% lauryldimethylamine oxide (LDAO, Fluka, Buchs, Switzerland), 3% heptanetriol (>98%, Sigma, St Louis, MO), 10 mM sodium phosphate pH 6.8, and 50 μM ubiquinone-2 (UQ2).

Soaking and mounting buffers contained 0.1% LDAO, 1% heptanetriol, 10 mM sodium phosphate, and 50 μM UQ2. Thin crystals (<100 μm) were removed from the mother liquor into a soak buffer at 2.4 M ammonium sulfate, 80 μM ferricyanide, and 20 μM ferrocyanide, then transferred to a buffer containing 2.4 M ammonium sulfate and 10 μM ethylenediaminetetraacetic acid (EDTA) for mounting. The presence of ferricyanide is required to oxidize the high-potential heme c_{559} (+380 mV) that would otherwise rereduce the special pair; the subsequent removal of ferricyanide is required because it is also an exogenous acceptor for the semiquinone Q_A^-.[40] Crystals were transferred from 1 mL of oxidizing soak buffer to a capillary filled with EDTA soak buffer for mounting. It was assumed that the volume of buffer inside the capillary was sufficiently greater than that of the crystal to reduce the concentration of ferricyanide to <1 μM.

Crystals were mounted in 1 mm X-ray capillaries (Glass #50, Hampton Research Inc., Laguna Niguel, CA). The capillary was filled with soak buffer but for a small gap of air close to the uncut end. The crystal was transferred into the buffer at the top of the capillary, which was then inverted, allowing the crystal (which is buoyant in the soak buffer) to rise inside the capillary to the internal meniscus near the capillary's end. The capillary was cut, and excess buffer was wicked from the crystal. A small slug of buffer and then mineral oil was introduced between the crystal and the cut end of the capillary, which was sealed with epoxy resin. The glue drew inward due to capillary action, and any excess was removed from the exterior, so that the sealed capillary containing the crystal could lie flat on a surface.

Capillaries were mounted on thin metal plates with a small hole (~200 μm) drilled in the center. The capillary was manipulated so as to align the crystal as close as possible to the metal surface and cover the hole. After both ends were fixed with model cement, further masking was accomplished with small strips of aluminum foil slipped between the capillary and the surface of the metal strip. Additional Al foil was used to form a top mask to restrict the angular acceptance of light through the sample. All manipulations were performed under a microscope fitted with a red filter. The microscope was fitted with a charge coupled device (CCD) camera and closed circuit television monitor, which allowed the entire process to be performed in minimal ambient light.

Spectra were collected on a high-performance single-beam microspectrophotometer at the Research School of Chemistry, Australian National University. This instrument has been previously described.[41] A 24-V, 150-W quartz−halogen bulb was used as the light source for a SPEX 1704 1-m Czerny−Turner single monochromator. Polarization optics and an 830-nm long-pass order-sorting glass filter preceded the sample chamber. The measuring light was focused in the chamber, and the sample was placed so that the pinhole was at this focus and the capillary vertical. Due to the tendency of RC crystals to grow to the longest dimension along their *c*-axis and hence align this way inside the capillary, the horizontal polarization corresponded to $E \perp z$, and the vertical polarization to $E \parallel z$. Light passing through the sample was refocused onto the detector, a 3-mm^2 thermo-electrically cooled InGaAs photodiode (Sciencetech, London, ON). The transmission signal was measured using a Stanford 510 lock-in amplifier and stored on a PC, which both scanned the spectrometer and controlled the lock-in via a general purpose interface bus.

To obtain accurate spectroscopic measurements on illumination-induced changes in *B. viridis*, we performed measurements on relatively thin crystals. The crystals were mounted in capillaries identical to those used for X-ray data collection. The illumination system used for crystallographic studies,[21] a Q-switched Nd:YAG dye laser at 635 nm with laser pulses being delivered by fiber optics and further collimated onto the crystal, could not be reproduced. Rather, a continuous wave (CW) HeNe laser (632.8 nm) was used to illuminate the sample at an angle of 60° to the measurement beam. Sample exposures were controlled by an electronic shutter and a second 830-nm long-pass filter placed in front of the InGaAs detector, which prevented any laser light reaching it. To precisely determine the optical changes due to the illumination of the crystal, we paid particular attention to the absorption of P^+ at 1300 nm. Monitoring this absorption band has two benefits. There is no absorbance in this region due to other pigments or the ground state of P itself, and the (actinic) measurement light in this region does not induce photoconversion of P.

Results

Figure 1 shows a near-infrared absorption difference spectrum of a reaction center crystal mounted in the manner described above, in the presence and absence of illumination from a CW HeNe laser. The P^+ absorption band has a λ_{max} of 1312 nm

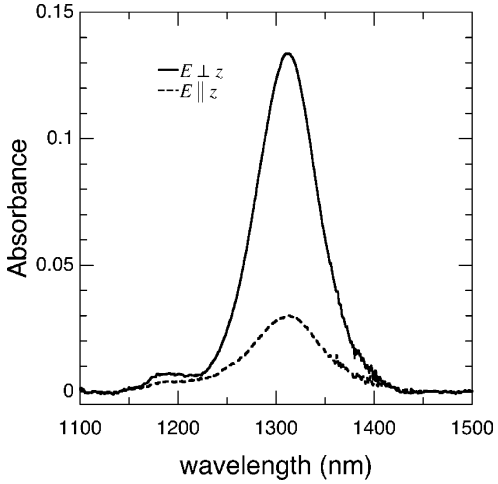

Figure 1. Near-infrared difference absorption spectrum of a *B. viridis* crystal illuminated with a 1-mW CW HeNe laser. Spectra were recorded from 1100 to 1500 nm at a resolution of 1 nm with a 1000-nm long-pass filter before the sample and a 1100-nm long-pass filter between the sample and the detector. The baseline was subtracted by fitting a cubic polynomial to data at 1100−1150 and 1450−1500 nm. The perpendicular polarization is depicted with an unbroken line, and the parallel polarization with a dashed line.

(7622 cm^{-1}) and a full width at half-maximum (fwhm) of 70 nm, with a vibronic sideband at 1190 nm. For a crystal of tetragonal symmetry, there are only two independent polarizations: the electric field vector perpendicular to the principal (fourfold) axis ($E \perp z$) or parallel to it ($E \parallel z$). The P^+ band is polarized perpendicular to the principal axis in the same manner as the primary donor itself at 970 nm, indicating only a small change in dipole moment from the ground state. This is in agreement with observations made for the *R. sphaeroides* reaction center[42] and the assignment of this band as arising from a triplet-coupled monomer absorption within a weakly coupled dimer.[43]

All further experiments were conducted on a second single crystal of dimensions 600 × 100 × 40 μm^2 (±10 μm as measured using a calibrated optical microscope). Figure 2a shows the visible absorption spectrum of this crystal in the two independent polarization states. The spectrum agrees well with that of Knapp et al.[35] The special pair P absorbs at a λ_{max} of 968.5 nm (10 330 cm^{-1}) and a fwhm of 78 nm. The accessory bacteriochlorophyll absorption at 830 nm is truncated by the stray light limit of the system for optical densities >2.5. Figure 2b shows a comparison of the calculated isotropic spectrum with a solution spectrum of solubilized RCs. (The slight red shift and increased absorbance of the 970-nm absorption in the solution spectrum is most likely due to the residual intact LH1−RC complexes in the preparation.) The calculated spectrum is in good agreement with the solution spectrum up to the stray light limit, including the bacteriopheophytin shoulder at 790 nm. Photoconversion of the P to P^+ can be quantitatively measured by measurements at 970 and 1300 nm. Additional verification of this procedure can be obtained by using the molar extinction coefficient for the primary donor, $\epsilon_{970} = 123 \pm 25$ mM^{-1} cm^{-1} [44] and the known concentration of RCs within the crystal lattice (8 per unit cell volume = 2.364 mM) to calculate the path length of the sample from the isotropic $A_{970} = 1.46$

$$b = 1.46 \div (123(\pm 25) \times 2.364) = 50 \pm 10\ \mu m$$

This is within the error of the smallest crystal dimension measured by the microscope. Finally, the actinic effect associated with the measuring light was determined by systematically reducing the intensity of the measurement beam and monitoring any change in the intensity of the P band A_{970}. We found no significant effect associated with the actinic light.

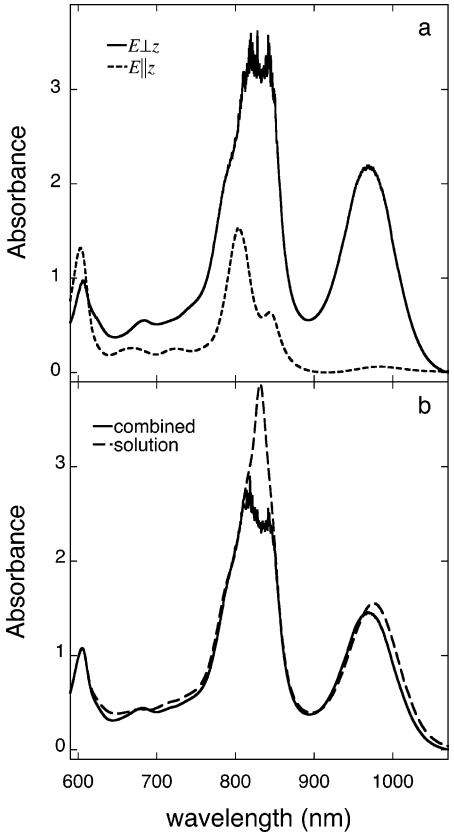

Figure 2. Visible/near-infrared absorption spectrum of a *B. viridis* crystal. Spectra were recorded from 590 to 1100 nm, at 0.5-nm resolution, and with a 550-nm prefilter and 0.1-mm entrance/exit slits. (a) The perpendicular polarization is depicted with an unbroken line, and the parallel polarization with a dashed line, absorbance relative to A_{1070}. (b) Calculated solution spectrum ($^2/_3A_\perp + {}^1/_3A_\parallel$, unbroken line) compared to the absorption spectrum of RCs in solution (dashed line).

Photoactivation of the crystal was achieved with a CW HeNe laser of incident power $P = 2.6 \pm 0.1$ mW. The laser beam was directed onto the sample, in the horizontal plane, at an angle of ~60° to the incident beam. The sample was exposed for a 10-s period, with neutral density filters used to attenuate the beam. At least three traces were recorded at each wavelength at each power level, starting at 26 nW (optical density (OD) 5 neutral density filter) up to the full laser power. Near-infrared spectra taken before, during, and after the power-saturation measurements are shown in Figure 3. The absorbencies of P and P^+ in these spectra are tabulated in Table 1. The first three traces (a−c) illustrate steady-state photoactivation at low powers, with partial bleaching of P and the simultaneous appearance of P^+. Steady-state charge separation is reversible at low powers. Trace d shows that all transient exposures during the power-saturation experiment were reversible. Trace e shows that continuous illumination at full laser power was capable of complete bleaching of P, although trace f shows that in this case a certain fraction of the bleach was irreversible (and a fraction of centers remained in the P^+ state).

Figure 4 shows the result of transient illumination of the crystal at differing laser powers, with the rise and decay of P^+, and the bleaching and recovery of P, monitored photometrically at 1300 and 970 nm, respectively. A total period of 500 s was

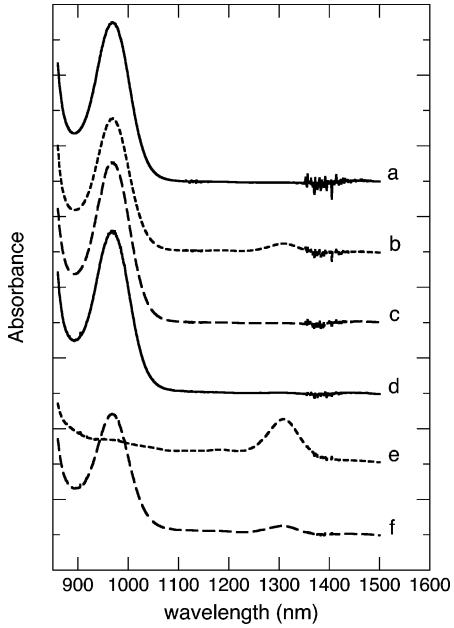

Figure 3. Near-infrared absorption spectra in the perpendicular polarization demonstrating incomplete, reversible photoactivation and complete, irreversible photoactivation. Spectral parameters: 860−1500 nm, 0.5-nm resolution, 830-nm prefilter, 0.1/0.2-mm entrance/exit slits, InGaAs detector, and 18-min acquisition time. (a) Dark spectrum, (b) continuous illumination 2.6×10^{-4} mW, (c) recovery, (d) dark after completion of power-saturation experiments, (e) continuous illumination at 2.6 mW, and (f) final spectrum.

TABLE 1: Steady-State Illumination

spectrum	A_{970}[a]	A_{1300}[a]
a	2.24	−0.031
b	1.87	0.107
c	2.25	−0.024
d	2.24	0.001
e	0.16	0.561
f	1.63	0.109

[a] $A_{970} = \log(I_{1100}/I_{970})$, $A_{1300} = \log(I_{1450}/I_{1300})$.

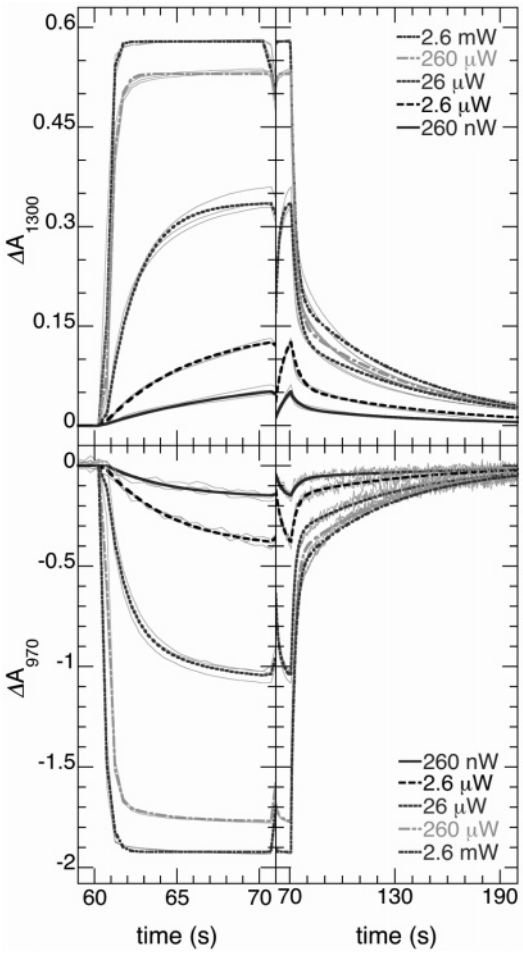

Figure 4. Photoactivation of a *B. viridis* RC crystal by illumination at 635 nm. The top panels show the rise (left) and decay (right) of P^+ at 1300 nm, and the bottom panels the bleach (left) and recovery (right) of P at 970 nm. The illuminating power was varied over 5 orders of magnitude; the fitted curve at each power and wavelength is the result of at least three independent measurements.

recorded at 0.5-s resolution for each trace to establish a dark baseline (measured 60 s prior to illumination) and return to that baseline after illumination. Figure 4 shows the rise of P^+ and the bleaching of P over the 10-s illumination period and the subsequent relaxation in the first 120 s after illumination.

Each trace can described by a piecewise function with 10 parameters: the initial intensity I_0, the start time for illumination t_0, a maximum intensity I_1 for theoretical steady-state illumination, two forward rate constants k_1 and k_2 and their ratio a, the end time for illumination t_1, and two rate constants for the decay to the ground state k_3 and k_4 and their ratio b. For intermediate laser powers, the parameters k_2 and a were necessary to adequately fit the spectrum; otherwise they were not used. For high laser powers, the times t_0 and t_1 were treated as variables rather than fixed values because the rise (and decay) of the signal was faster than the time resolution of the data collection; hence the uncertainty in the value of t_0 and t_1 led to a poor estimate of the rate constant. (In this case t_0 and t_1 were constrained to lie within the time separating the two relevant data points.)

The data were divided into three segments—before, during, and after illumination—fit in succession; the parameters fit within each segment were applied as fixed values in the next. In each segment the individual traces were simultaneously fit to the model by the general nonlinear (Levenberg−Marquardt) fitting algorithm implemented in the computer program ORIGIN. First the data $t < t_0$ were fit to give the value of I_0. Next the data $t_0 < t < t_1$ were fit to the function $\log I(t) = (\log I_1 - \log I_0)(1 - a\, e^{-k_1(t-t_0)} - (1 - a)e^{-k_2(t-t_0)})$ to give the values of I_1, k_1, k_2, and a for intermediate laser powers and t_0 for high laser powers. Finally, the data $t > t_1$ were fit to the function $\log I(t) = (\log I_1 - \log I_0)(b\, e^{-k_3(t-t_0)} + (1 - b)e^{-k_4(t-t_0)})$ to give the values of k_3, k_4, b, and t_1 for high laser powers. The parameters for the fit are listed in Table 2.

From this fitting procedure, the absorbance changes at 970 and 1300 nm as a function of laser power were obtained and are listed in Table 3. For the bleaching of P, the steady-state illumination (Figure 3 and Table 1) allows us to obtain a good estimate of the maximum absorbance change, $\Delta A_{970}(\max) = 2.24 - 0.16 = 2.08$. At 1300 nm, however, we cannot be certain that all centers in which P is bleached give rise to P^+. In fact this is definitely not the case for trace e of Figure 3, because the bleaching of P is not fully reversible, and the absorbance increase at 1300 nm ($\Delta A = 0.56$) is less than that observed in the transient illumination at full power (0.58). However, we may use the reversible photoactivation at low power (Figures 4a−c) to estimate the absorbance of P to P^+. The change in absorbance at low power is $2.24 - 1.87 = 0.37$ at 970 nm and 0.11 at 1300 nm.[45] Hence, we may estimate the absorbance for 100% photoactivation to be $2.08 \times (0.11/0.37) = 0.62$ at 1300 nm. The resulting fraction of photoactivation as a function of

TABLE 2: Transient Illumination Fitting Parameters

power	log I_0	log I_1	k_1	k_2	a	k_3	k_4	b
				970 nm				
260 nW	−3.8876	−3.728	0.26		1	0.22	0.0094	0.60
	(0.0007)	(0.009)	(0.03)			(0.02)	(0.0003)	(0.01)
2.6 μW	−4.241	−3.82	0.24		1	0.32	0.0145	0.601
	(0.001)	(0.01)	(0.02)			(0.02)	(0.0003)	(0.008)
26 μW	−4.242	−3.16	0.95	0.24	0.70	0.50	0.0165	0.672
	(0.001)	(0.08)	(0.32)	(0.30)	(0.27)	(0.01)	(0.0002)	(0.003)
260 μW	−4.227	−2.45	3.71	0.38	0.94	0.49	0.0169	0.743
	(0.001)	(0.02)	(0.77)	(0.49)	(0.05)	(0.01)	(0.0001)	(0.002)
2.6 mW	−4.208	−2.286	3.02		1	0.45	0.0184	0.724
	(0.001)	(0.003)	(0.07)			(0.01)	(0.0002)	(0.002)
				1300 nm				
260 nW	−1.52986	−1.606	0.11		1	0.188	0.01224	0.469
	(0.00005)	(0.008)	(0.02)			(0.004)	(0.00006)	(0.002)
2.6 μW	−1.76760	−1.916	0.19		1	0.217	0.01204	0.542
	(0.00001)	(0.004)	(0.01)			(0.004)	(0.00008)	(0.002)
26 μW	−1.80019	−2.136	0.54		1	0.296	0.01273	0.605
	(0.00005)	(0.003)	(0.02)			(0.006)	(0.00008)	(0.002)
260 μW	−1.80585	−2.336	2.78		1	0.403	0.01382	0.696
	(0.00002)	(0.002)	(0.14)			(0.004)	(0.00006)	(0.001)
2.6 mW	−1.80889	−2.388	4.94		1	0.415	0.01467	0.658
	(0.00009)	(0.0004)	(0.80)			(0.006)	(0.00008)	(0.001)

TABLE 3: Photoactivation vs Laser Power

	970 nm		1300 nm	
energy	$\lvert\Delta A\rvert$	$\lvert\Delta A/A_{max}\rvert$	$\lvert\Delta A\rvert$	$\lvert\Delta A/A_{max}\rvert$
2.6 μJ	0.148	0.07	0.051	0.08
26 μJ	0.379	0.18	0.126	0.20
260 μJ	1.037	0.50	0.334	0.54
2.6 mJ	1.768	0.85	0.530	0.85
26 mJ	1.922	0.92	0.578	0.93

laser power (listed as a fraction in Table 3 and shown as a percentage in Figure 5) is in excellent agreement between the two wavelengths across the 5 orders of magnitude measured. The crystal was >90% photoactivated at full power, and 0.26 mW was sufficient to achieve 50% photoactivation.

Discussion

The extent of photoactivation observed in the crystal ranged from 7% (2.6 μJ actinic light) to 93% (26 mJ actinic light). The measurements also provide information on the rates of formation and decay of the charge-separated state in the crystal.

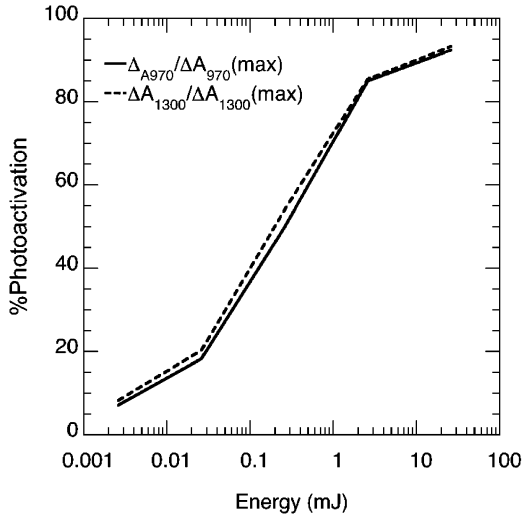

Figure 5. Photoactivation as a function of laser power. The maximum ΔA from the fit to data in Figure 4 was divided by the estimated absorbance for 100% photoactivation, equal to 2.08 absorbance units for P and 0.62 absorbance units for P^+ (Table 1).

These observations relate to two assumptions made by Baxter et al.,[21] (i) that the actinic light is sufficient to achieve significant photoactivation within the crystal and (ii) that the charge-separated state decays within the dark period between actinic exposures.

To relate our results to assumption i, we must account for the difference in thickness between the crystal used in this study and those used by Baxter et al.[21] The crystal in the current study was mounted with dimensions of 40 μm in the path of the measuring beam and 100 μm perpendicular to that path. Given the angle of incidence for the actinic light, a reasonable estimate for its path length through the crystal is a diagonal from the front corner of the crystal to the center of its rear face, i.e., $(40^2 + 50^2)^{1/2} = 65$ μm. In Baxter et al.,[21] the largest crystal used had dimensions 200 × 200 μm^2 and was illuminated by two counter-propagating laser pulses of 1−2 mJ with a 45° angle of incidence, yielding an effective path length of 215 μm. The path length corresponding to an optical density of 1 at 630 nm in *B. viridis* RC crystals is $b = 140$ μm. Hence, the crystal in this study is comparable to the last third of the optical path through the largest crystal in Baxter et al.[21] if the energy of the actinic light in Figure 5 is reduced by a factor of 10. Accordingly, the laser energy used by Baxter et al.[21] (1−2 mJ) would have produced ~80% photoactivation within the first third of its optical path and ~40% within the last third of its effective optical path. We infer that 50% overall photoactivation is a conservative estimate for the thickest crystal used in Baxter et al.[21]

In previous time-resolved crystallographic studies of the photolysis of CO from myoglobin, the extent of photoactivation was determined to be 50%.[26] In a freeze-trapping study in *R. sphaeroides* RCs, the extent of photoactivation was estimated to be 95%.[7] A previous calculation assuming 100% quantum yield in *B. viridis* RC crystals suggested that the laser should produce 97% photoactivation, but this estimate drops to 50% if the quantum yield is assumed to be only 10%.[21] Various factors such as misalignment of the laser, nonuniform distribution of energy in the incident beam, photons not absorbed due to polarization along the *z*-axis of the crystal, and scattering by the capillary, mother liquor, or precipitated protein/salt on the crystal surface can account for an effective quantum yield of 10%. Nevertheless, the principal assumption of the

time-resolved crystallographic experiment that the laser pulse may produce significant photoactivation in the crystal is valid.

To relate our results to assumption ii, we must compare the half-life of the charge-separated state observed to the dark period between laser pulses used by Baxter et al.[21] There are two distinct kinetic phases in the decay, with similar rates and amplitudes obtained at both wavelengths. The first, accounting for ~70% of the decay, has rate constant $k_3 = 0.44 \pm 0.04$ s^{-1} (from both wavelengths at the two highest laser powers), $t_{1/2} = 1.6 \pm 0.1$ s. This corresponds to the charge recombination of the $P^+Q_B^-$ state. The charge-recombination reaction has a half-life of ~100 ms in aqueous solution, but the rate slows to $t_{1/2} = 1$ s in the presence of 2 M NaCl,[46] so our observed rate is reasonable in the presence of 2.6 M $(NH_4)_2SO_4$.

In Baxter et al.,[21] the light image was collected within milliseconds of the laser pulse, the dark image ~3 s later, and the next light image ~3 s later again; this timing was based on the readout time of the ADSC Quantum Q4 detector. The 11 images were collected in succession at different angles through 90°, then the goniometer was reset (~1 min), and a second set of 11 images was collected at interspersing angles. In terms of the observed charge-recombination rate, the dark image was collected only two half-lives after the light image and so would contain ~25% of the light state. The dark period of 6 s corresponds to 3.75 half-lives, so the crystal at the time of the next laser pulse contained 92.6% of the centers in the dark state. Iterating this over the series of 11 images, a photostationary state would develop in 50% of centers after 9 images, with the final light image containing 43% of the centers in the dark state. The photostationary state would dissipate during the resetting of the goniometer.

A second, much slower, rate of decay was also observed. This phase, comprising ~30% of the total amplitude, has the rate constant $k_4 = 0.016 \pm 0.002$ s^{-1} (from both wavelengths at the two highest laser powers), $t_{1/2} = 43 \pm 5$ s. A long-lived P^+ state could be very problematic for the experiment of Baxter et al.[21] because no appreciable decay would occur during the dark period of 6 s. Depending on the origin of the long-lived state, each laser pulse could produce an additional 30% of centers trapped in the P^+ state, and this hypothetical photostationary state would be complete after 3 images had been collected. Hence, the assumption of decay of the charge separated state by Baxter et al.[21] would not be valid.

The cause of the long-lived P^+ state is uncertain. Possible mechanisms may involve oxidation of the special pair by an exogenous oxidant in the mother liquor,[40,47] interprotein redox reactions mediated by a diffusible species in the mother liquor, a subpopulation of centers containing Q_B in the semiquinone state,[5,9] or some large-scale structural change to a fraction of centers in the sample that leads to a stabilization of the charge-separated state. It is also uncertain whether any difference between the spectroscopic studies and the time-resolved experiment, such as the less stringent soak conditions or the extended period of illumination, may be relevant to this long-lived P^+ state. Recent spectroscopic and structural evidence has been reported regarding the accumulation of a long-lived charge-separated state in *R. sphaeroides* RCs exposed to bright light for extended periods.[48,49]

Additional spectroscopic and time-resolved crystallographic experiments are required to determine the cause of the long-lived P^+ state and its effect on pump−probe experiments performed in *B. viridis* RC crystals. The problem of a long-lived charge-separated state is readily solved by extending the dark period of the time-resolved X-ray experiment. A dark period of 2 min would be adequate for >95% relaxation of the long-lived P^+ state. The dark image should be collected after this time, immediately preceding the next light image. The long-lived P^+ might be reduced by (i) altering the composition of the mother liquor to reduce the concentration condition of potential soluble donors/acceptors or (ii) reducing the rate of exogenous oxidation/reduction, for instance, by increasing the pH of the mother liquor.[40] Complications from an oxidizing soak buffer would be avoided if time-resolved experiments were performed with the *R. sphaeroides* RC, which does not possess a tightly bound cytochrome subunit.

Although off-line microspectroscopy of thin crystals was most appropriate to measure the extent of photoactivation of RC crystals, near-infrared in situ microspectroscopy could be performed on larger crystals for the purposes of kinetic measurements, owing to the low background and lower molar extinction coefficient of P^+. The use of in situ microspectroscopy would remove any potential artifacts due to different sample preparation, sample size, or method of illumination. Such experiments should be used to guide the timing of the pump−probe crytallographic experiment. In situ microspectroscopy may also provide information on the effects of radiation damage during the crystallographic experiment, which may also be a significant factor in structural studies of the reaction center.[50,51]

Although the time-resolved experiment of Baxter et al.[21] failed to observe any significant motion of the quinone, some evidence of structural changes was observed in crystals frozen in the light and dark,[50] although these are complicated by the effects of radiation damage. Recently a large-scale conformation change was reported in the *R. sphaeroides* RC as a result of extended light adaption.[49] These observations provide further impetus for further time-resolved studies and the need to carefully control the conditions of crystallographic experiments.

Improvements aimed at further increasing the extent of photoactivation in the crystal should be considered. Additional sources of illumination at 90° to the two in Baxter et al.[21] or adopting tetrahedral symmetry should not only improve the overall extent of photoactivation but also decrease the systematic error due to variation in (i) the extent of photoactivation in different sized crystals, (ii) the extent of photoactivation between crystals of different sizes, (iii) the extent of photoactivation with rotation of the crystal due to varying optical path lengths, (iv) the absorbance with rotation of the crystal due to polarization of the electric dipole transition moment, and (v) the temperature gradient within the crystal produced by differential absorption of light. It would also allow the use of larger crystals, which would be advantageous for weakly scattering samples such as the RC.

Photoactivation may also be more efficient at a different wavelengths of illumination. The wavelength of minimum optical density in the visible region for the *B. viridis* RC is 630 nm. Although this assists transmission of light through the sample, it is a problematic wavelength because of absorption from multiple chromophores in the RC at that wavelength. RCs that have already undergone charge separation will absorb photons nonproductively. An alternative is to illuminate the RC at the wavelength of maximum absorption by the special pair, 970 nm. Although the optical density of the sample in this region is much greater, the only significant absorbing species is P, which upon absorption undergoes charge separation and becomes P^+, ceasing to absorb at the wavelength of illumination. Hence, no photons are "wasted". Spectroscopic experiments

such as those reported here can be used to test this hypothesis by monitoring the generation of the special pair cation at 1300 nm.

With continual improvement in experimental design and successful analysis of time-resolved crystallographic data, the method shall be extended to other weakly scattering and optically dense samples such as the RC, for instance, photosystem II. This study illustrates the feasibility of efficient photoactivation of such optically dense samples but also the need to characterize the kinetics of reactions in the crystalline state, which may differ from those in solution due to the particular state of the protein or the composition of the mother liquor.

Acknowledgment. This work was supported by the Department of Energy (Grant No. FG02-96ER14675 to J.R.N.). R.H.G.B. was supported by the Burroughs Wellcome Fund Interfaces in Science Program (Grant No. 1001774) at the University of Chicago. The Burroughs-Wellcome fellowship also allowed for the purchase of the InGaAs photodiode used. Dr. Nina Ponomarenko, Dr. Sindra Årskold-Peterson, and Keith Jackman provided assistance in conducting these experiments.

References and Notes

(1) Deisenhofer, J.; Michel, H. *Annu. Rev. Cell Biol.* **1991**, *7*, 1.

(2) Gray, H. B.; Winkler, J. R. *Q. Rev. Biophys.* **2003**, *36*, 341.

(3) Hoff, A. J.; Deisenhofer, J. *Phys. Rep.* **1997**, *287*, 2.

(4) Deisenhofer, J.; Epp, O.; Miki, K.; Huber, R.; Michel, H. *Nature* **1985**, *318*, 618.

(5) Ermler, U.; Fritzsch, G.; Buchanan, S. K.; Michel, H. *Structure* **1994**, *2*, 925.

(6) Lancaster, C. R. D.; Michel, H. *Structure* **1997**, *5*, 1339.

(7) Stowell, M. H. B.; McPhillips, T. M.; Rees, D. C.; Soltis, S. M.; Abresch, E. C.; Feher, G. *Science* **1997**, *276*, 812.

(8) McAuley, K. E.; Fyfe, P. K.; Ridge, J. P.; Isaacs, N. W.; Cogdell, R. J.; Jones, M. R. *Proc. Natl. Acad. Sci. U.S.A.* **1999**, *96*, 14706.

(9) McAuley, K. E.; Fyfe, P. K.; Ridge, J. P.; Cogdell, R. J.; Isaacs, N. W.; Jones, M. R. *Biochemistry* **2000**, *39*, 15032.

(10) Axelrod, H. L.; Abresch, E. C.; Paddock, M. L.; Okamura, M. Y.; Feher, G. *Proc. Natl. Acad. Sci. U.S.A.* **2000**, *97*, 1542.

(11) Kuglstatter, A.; Ermler, U.; Michel, H.; Baciou, L.; Fritzsch, G. *Biochemistry* **2001**, *40*, 4253.

(12) Pokkuluri, P. R.; Laible, P. D.; Deng, Y. L.; Wong, T. N.; Hanson, D. K.; Schiffer, M. *Biochemistry* **2002**, *41*, 5998.

(13) Fritzsch, G.; Koepke, J.; Diem, R.; Kuglstatter, A.; Baciou, L. *Acta Crystallogr., Sect. D* **2002**, *58*, 1660.

(14) Pokkuluri, P. R.; Laible, P. D.; Crawford, A. E.; Mayfield, J. F.; Yousef, M. A.; Ginell, S. L.; Hanson, D. K.; Schiffer, M. *FEBS Lett.* **2004**, *570*, 171.

(15) Xu, Q.; Axelrod, H. L.; Abresch, E. C.; Paddock, M. L.; Okamura, M. Y.; Feher, G. *Structure* **2004**, *12*, 703.

(16) Baxter, R. H. G.; Seagle, B.-L.; Ponomarenko, N.; Norris, J. R. *Acta Crystallogr., Sect. D* **2005**, *61*, 605.

(17) Grafton, A. K.; Wheeler, R. A. *J. Phys. Chem. B* **1999**, *103*, 5380.

(18) Okamura, M. Y.; Paddock, M. L.; Graige, M. S.; Feher, G. *Biochim. Biophys. Acta* **2000**, *1458*, 148.

(19) Kleinfeld, D.; Okamura, M. Y.; Feher, G. *Biochemistry* **1984**, *23*, 5780.

(20) Graige, M. S.; Feher, G.; Okamura, M. Y. *Proc. Natl. Acad. Sci. U.S.A.* **1998**, *95*, 11679.

(21) Baxter, R. H. G.; Ponomarenko, N.; Šrajer, V.; Pahl, R.; Moffat, K.; Norris, J. R. *Proc. Natl. Acad. Sci. U.S.A.* **2004**, *101*, 5982.

(22) Breton, J. *Biochemistry* **2004**, *43*, 3318.

(23) Breton, J.; Boullais, C.; Mioskowski, C.; Sebban, P.; Baciou, L.; Nabedryk, E. *Biochemistry* **2002**, *41*, 12921.

(24) Remy, A.; Gerwert, K. *Nat. Struct. Biol.* **2003**, *10*, 637.

(25) Šrajer, V.; Ren, Z.; Teng, T.-Y.; Schmidt, M.; Ursby, T.; Bourgeois, D.; Pradervand, C.; Schildkamp, W.; Wulff, M.; Moffat, K. *Biochemistry* **2001**, *40*, 13802.

(26) Šrajer, V.; Teng, T.-Y.; Ursby, T.; Pradervand, C.; Ren, Z.; Adachi, S.-I.; Schildkamp, W.; Bourgeois, D.; Wulff, M.; Moffat, K. *Science* **1996**, *274*, 1726.

(27) Anderson, S.; Šrajer, V.; Pahl, R.; Rajagopal, S.; Schotte, F.; Anfinrud, P.; Wulff, M.; Moffat, K. *Structure* **2004**, *12*, 1039.

(28) Rajagopal, S.; Anderson, S.; Šrajer, V.; Schmidt, M.; Pahl, R.; Moffat, K. *Structure* **2005**, *13*, 55.

(29) Ren, Z.; Perman, B.; Šrajer, V.; Teng, T.-Y.; Pradervand, C.; Bourgeois, D.; Schotte, F.; Ursby, T.; Kort, R.; Wulff, M.; Moffat, K. *Biochemistry* **2001**, *40*, 13788.

(30) Pearson, A. R.; Mozzarelli, A.; Rossi, G. L. *Curr. Opin. Struct. Biol.* **2004**, *14*, 656.

(31) Chen, Y.; Šrajer, V.; Ng, K.; Legrand, A.; Moffat, K. *Rev. Sci. Instrum.* **1994**, *65*, 1506.

(32) Hadfield, A.; Hajdu, J. *J. Appl. Crystallogr.* **1993**, *26*, 839.

(33) Sakai, K.; Matsui, Y.; Kouyama, T.; Shiro, Y.; Adachi, S. *J. Appl. Crystallogr.* **2002**, *35*, 270.

(34) Stowell et al.[7] report a power-saturation curve for a 200-μm-thick crystal of the RC of *R. sphaeroides* measured at 480 nm. This is possible because the absorbance of the *R. sphaeroides* RC at 480 nm is significantly less than that of *B. viridis*, by our estimation 20 vs 116 $mM^{-1}cm^{-1}$, respectively. Given the local concentration of the RC within tetragonal crystals of *R. sphaeroides* (5.0 mM) and *B.* viridis (2.3 mM) and ignoring polarization effects, the optical density of a 200-μm crystal of *R. sphaeroides* at 480 nm is 1 while the optical density of a 200-μm crystal of *B. viridis* at 480 nm is >5.

(35) Knapp, E. W.; Fischer, S. F.; Zinth, W.; Sander, M.; Kaiser, W.; Deisenhofer, J.; Michel, H. *Proc. Natl. Acad. Sci. U.S.A.* **1985**, *82*, 8463.

(36) Zinth, W.; Kaiser, W.; Michel, H. *Biochim. Biophys. Acta* **1983**, *723*, 128.

(37) Weaver, P. F.; Wall, J. D.; Gest, H. *Arch. Microbiol.* **1975**, *105*, 207.

(38) Fritzsch, G. *Methods Enzymol.* **1998**, *297*, 57.

(39) Michel, H. *J. Mol. Biol.* **1982**, *158*, 567.

(40) Shopes, R. J.; Wraight, C. A. *Biochim. Biophys. Acta* **1986**, *848*, 364.

(41) Krausz, E. *Aust. J. Chem.* **1993**, *46*, 1041.

(42) Stocker, J. W.; Hug, S.; Boxer, S. G. *Biochim. Biophys. Acta* **1993**, *1144*, 325.

(43) Reimers, J. R.; Hush, N. S. *J. Am. Chem. Soc.* **1995**, *117*, 1302.

(44) Clayton, R. K.; Clayton, B. J. *Biochim. Biophys. Acta* **1978**, *501*, 478.

(45) Strictly speaking, the ratio should be derived from integration over both bands to apply the conservation of oscillator strength, but since the fwhm of the two absorption bands is very similar and the short-wavelength edge of P is not well-measured due to overlap with the accesory BChl, this estimate will suffice.

(46) Gao, J. L.; Shopes, R. J.; Wraight, C. A. *Biochim. Biophys. Acta* **1991**, *1056*, 259.

(47) An exogenous oxidant may not fully account for the long-lived P^+ state because of the high local concentration of RCs within the crystal.

(48) Andréasson, U.; Andréasson, L.-E. *Photosynth. Res.* **2003**, *75*, 223.

(49) Katona, G.; Snijder, A.; Gourdon, P.; Andréasson, U.; Hansson, Ö.; Andréasson, L.-E.; Neutze, R. *Nat. Struct. Mol. Biol.* **2005**, *12*, 630.

(50) Baxter, R. H. G.; Seagle, B.-L.; Ponomarenko, N.; Norris, J. R. *J. Am. Chem. Soc.* **2004**, *126*, 16728.

(51) Yano, J.; Kern, J.; Irrgang, K.-D.; Latimer, M. J.; Bergmann, U.; Glatzel, P.; Pushkar, Y.; Biesiadka, J.; Loll, B.; Sauer, K.; Messinger, J.; Zouni, A.; Yachandra, V. *Proc. Natl. Acad. Sci. U.S.A.* **2005**, *102*, 12047.